Environmental Research Letters

LETTER • **OPEN ACCESS**

Detection of fossil fuel emission trends in the presence of natural carbon cycle variability

To cite this article: Yi Yin *et al* 2019 *Environ. Res. Lett.* **14** 084050

View the article online for updates and enhancements.

This content was downloaded from IP address 131.215.70.224 on 16/12/2019 at 19:07

Environmental Research Letters

LETTER

Detection of fossil fuel emission trends in the presence of natural carbon cycle variability

Yi Yin[1,2], Kevin Bowman[1,3], A Anthony Bloom[1] and John Worden[1]

[1] Jet Propulsion Laboratory, California Institute of Technology, Pasadena, CA, United States of America
[2] Division of Geological and Planetary Sciences, California Institute of Technology, Pasadena, CA, United States of America
[3] Joint Institute for Regional Earth System Science and Engineering, University of California, Los Angeles, CA, United States of America

E-mail: yiyin@caltech.edu

Keywords: fossil fuel emissions, trend detection, CO_2 monitor, carbon cycle

Supplementary material for this article is available online

OPEN ACCESS

RECEIVED
12 March 2019

REVISED
6 June 2019

ACCEPTED FOR PUBLICATION
28 June 2019

PUBLISHED
14 August 2019

Original content from this work may be used under the terms of the Creative Commons Attribution 3.0 licence.

Any further distribution of this work must maintain attribution to the author(s) and the title of the work, journal citation and DOI.

Abstract

Atmospheric CO_2 observations have the potential to monitor regional fossil fuel emission ($FFCO_2$) changes to support carbon mitigation efforts such as the Paris Accord, but they must contend with the confounding impacts of the natural carbon cycle. Here, we quantify trend detection time and magnitude in gridded total CO_2 fluxes—the sum of $FFCO_2$ and natural carbon fluxes—under an idealized assumption that monthly total CO_2 fluxes can be perfectly resolved at a $2^\circ \times 2^\circ$ resolution. Using Coupled Model Intercomparison Project 5 (CMIP5) 'business-as-usual' emission scenarios to represent $FFCO_2$ and simulated net biome exchange (NBE) to represent natural carbon fluxes, we find that trend detection time for the total CO_2 fluxes at such a resolution has a median of 10 years across the globe, with significant spatial variability depending on $FFCO_2$ magnitude and NBE variability. Differences between trends in the total CO_2 fluxes and the underlying $FFCO_2$ component highlight the role of natural carbon cycle variability in modulating regional detection of $FFCO_2$ emission trends using CO_2 observations alone, particularly in the tropics and subtropics where mega-cities with large populations are developing rapidly. Using CO_2 estimates alone at such a spatiotemporal resolution can only quantify fossil fuel trends in a few places—mostly limited to arid regions. For instance, in the Middle East, $FFCO_2$ can explain more than 75% of the total CO_2 trends in ~70% of the grids, but only ~20% of grids in China can meet such criteria. Only a third of the 25 megacities we analyze here show total CO_2 trends that are primarily explained (>75%) by $FFCO_2$. Our analysis provides a theoretical baseline at a global scale for the design of regional $FFCO_2$ monitoring networks and underscores the importance of estimating biospheric interannual variability to improve the accuracy of $FFCO_2$ trend monitoring. We envision that this can be achieved with a fully integrated carbon cycle assimilation system with explicit constraints on $FFCO_2$ and NBE, respectively.

1. Introduction

Current estimates of fossil fuel CO_2 emissions ($FFCO_2$) rely primarily on self-reported energy data from individual countries (IPCC 2013). Despite efforts to improve emission inventories, there is an increase in both relative and absolute errors in global $FFCO_2$ emissions because emissions are rising faster in nations with less accurate estimates (Andres *et al* 2014). To support individual countries' objectives for the Paris Agreement, atmospheric observations of CO_2 have the potential to provide an independent assessment of reported $FFCO_2$ emissions and associated trends (Peters *et al* 2017b, Battersby 2018). However, these observations provide constraints on the net contribution of both anthropogenic and natural sources and sinks. The annual atmospheric CO_2 growth rate owing to $FFCO_2$ is reduced by roughly a half due to ocean and land sinks, with the latter exhibits significant interannual variability (IAV) (Le Quéré *et al* 2018, Sellers *et al* 2018). This IAV is one of the primary confounding factors in the attribution of changes in $FFCO_2$ based on CO_2 concentrations.

© 2019 The Author(s). Published by IOP Publishing Ltd

Historically, global surface networks were designed to study ecosystem CO_2 fluxes (i.e., net biome exchange (NBE)) measuring CO_2 far away from urban locations. Atmospheric simulations of these observations relied upon 'bottom-up' inventories for $FFCO_2$ (Gurney *et al* 2002, Rödenbeck *et al* 2003, Peters *et al* 2007, Chevallier *et al* 2010, Francey *et al* 2013, Peylin *et al* 2013, Liu *et al* 2014, Gaubert *et al* 2019) to account for increases in background CO_2. With increasing surface observations in urban regions (McKain *et al* 2012, Staufer *et al* 2016, Turner *et al* 2016, Wu *et al* 2016, 2018, Verhulst *et al* 2017, Mitchell *et al* 2018) and the advent of satellite constellation dedicated to carbon gas measurements (O'Brien *et al* 2016, Pillai *et al* 2016, Broquet *et al* 2018, Crisp 2018), atmospheric CO_2 concentrations will be measured with much higher precision and resolution than before (Battersby 2018), with greater potential to distinguish natural and anthropogenic contributions. Nevertheless, the attribution of temporal-spatial variations in the atmospheric CO_2 concentration to anthropogenic emission trends is fundamentally limited by the balance of natural and anthropogenic variability and magnitude (National Research Council *et al* 2010, Shiga *et al* 2014).

One approach is to focus on limited domains where anthropogenic CO_2 emissions dominate CO_2 variability. For example, urban regions contribute to more than 70% of the global $FFCO_2$ emissions and are likely to increase as metropolitan areas are projected to grow (Duren and Miller 2012, Hutyra *et al* 2014), making them an especially attractive target for $FFCO_2$ monitoring. Urban CO_2 monitoring networks estimate city-scale $FFCO_2$ emissions using high-frequency measurements of CO_2 gradients between emitting sources and surrounding suburbs (McKain *et al* 2012, Lauvaux *et al* 2016, Staufer *et al* 2016, Wu *et al* 2016, Verhulst *et al* 2017, Mitchell *et al* 2018). On the other hand, space-borne column-integrated CO_2 (X_{CO2}) mixing ratio observations are also shown to be sensitive to CO_2 enhancements over megacity 'urban domes', e.g. Los Angeles (Kort *et al* 2012, Schwandner *et al* 2017) or power plants (Nassar *et al* 2017). However, the isolation of local $FFCO_2$ emission sources using such methods depend on CO_2 observations with relatively low and stable biosphere influences such as in arid regions.

Globally, extended urban landscapes exhibit considerable heterogeneity with a mosaic of residential, transportation, industrial, vegetation and agriculture areas, which may be situated in complex terrain. Wu *et al* (2018) showed that for Indianapolis, which has flat terrain but with similar magnitudes of biogenic and anthropogenic CO_2 fluxes, a CO_2 observation network of up to 12 sites at the city scale is not able to constrain $FFCO_2$ emissions effectively. The Indianapolis case indicates that the relative contribution from $FFCO_2$ and NBE to the total CO_2 has a direct impact on the accuracy of estimating $FFCO_2$. Consequently, any attempt to scale these city-scale case studies globally will need to account for this contribution and how it changes in space and time. Moreover, it is unclear if or when surface and aircraft measurement system would be deployed globally (e.g. Lagos, Moscow, Ho Chi Minh City).

Satellite remote sensing measurements with global coverage have been available for nearly a decade (Buchwitz *et al* 2018) with an increasing constellation that will include geostationary sounders (Polonsky *et al* 2014, Rayner *et al* 2014), which could provide critical constraints on the global time series of total CO_2 fluxes. It is unclear, however, how that time series will relate to the underlying $FFCO_2$ emissions at those scales. To that end, we focus on two factors here: (1) how long it takes for a significant trend to emerge in the total CO_2 fluxes, noted as detection time, given the confounding impact of NBE variability across the globe, and (2) the relationship between trends in the total CO_2 fluxes and trends in the $FFCO_2$ at each grid. In order to isolate the impact of the intrinsic variability of NBE from the accuracy and precision of a particular observing system, we make an important assumption that monthly total CO_2 flux time series could be perfectly known at a $2^\circ \times 2^\circ$ resolution. This corresponds to an idealized atmospheric CO_2 observing and attribution system that can fully solve monthly gridded carbon fluxes at such a resolution with a perfect transport model and sufficient CO_2 measurements. Consequently, these results are an upper bound in the detection time and accuracy of the trends at such a temporal and spatial resolution.

2. Data and method

2.1. CMIP5 emsRCP8.5 simulations

We use synthetic total CO_2 fluxes by combining $FFCO_2$ emissions under a 'business-as-usual' scenario, commonly noted as emsRCP8.5 (Taylor *et al* 2012), and corresponding emission-driven simulations of biospheric carbon fluxes—denoted as NBE—from the Coupled Model Intercomparison Project 5 (CMIP5, https://esgf-node.llnl.gov/search/cmip5/). The mean annual global $FFCO_2$ during 2005–2015 in emsRCP8.5 is 9.24 ± 0.74 PgC yr^{-1}, which agrees well with the emission inventories suggesting 9.22 ± 0.56 PgC yr^{-1} (Le Quéré *et al* 2016) (figure 1(a)). To mitigate some known model biases in the CMIP5 carbon-climate feedback mechanisms that manifest as unrealistic trends in the land carbon sink (Friedlingstein *et al* 2014, Hoffman *et al* 2014), we applied a model selection based on the agreement between simulated CO_2 growth rate and the observed changes during 2005–2015 (see supplementary text 1 online at stacks.iop.org/ERL/14/084050/mmedia).

Four models are included for further analysis, namely BNU-ESM, HadGEM2-ES, IPSL-CM5A-LR, and MPI-ESM-LR. The resulting model ensemble provides an uncertainty estimate of NBE fluxes. All

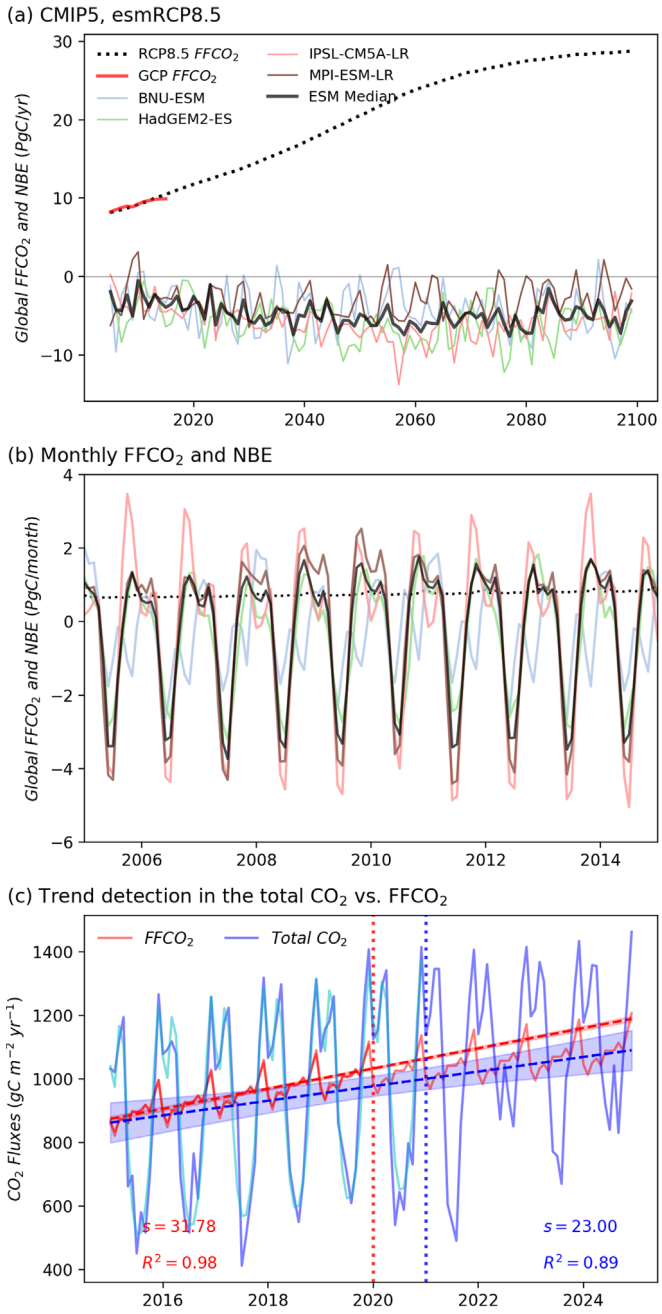

Figure 1. Time series of global fossil fuel CO_2 emission ($FFCO_2$) and net biome emission (NBE). (a) Global annual $FFCO_2$ and NBE simulated by the four models we use from CMIP5 esmRCP8.5 ensembles from 2005 to 2100. Dotted black lines represent FF emissions along with GCP estimates shown in red; color-coded lines represent individual ESM while black solid line represents the median of the selected ESMs. (b) Global monthly $FFCO_2$ and NBE for the period 2005–2015. The monthly $FFCO_2$ emissions are represented by the dotted-black line, which has a small seasonal cycle relative to NBE shown in color-coded lines. The added annual total emissions are shown in (a). (c) Monthly $FFCO_2$ and total CO_2 fluxes in the model grid Beijing locates. The blue line shows the monthly time series of the total CO_2 fluxes, the vertical dotted blue line indicates the trend detection time, the corresponding trend is shown in dashed-blue line. The cyan line shows the modeled seasonal cycle as represented by equation (2), and the shaded areas show the 95% confidence interval. Corresponding results for the $FFCO_2$ are shown in red.

models are resampled to $2^\circ \times 2^\circ$. This spatial resolution is limited by current global ESM simulations, but at the same time, equivalent to our current global inversions (Gurney *et al* 2002, Rödenbeck *et al* 2003, Peters *et al* 2007, Chevallier *et al* 2010, Francey *et al* 2013, Peylin *et al* 2013, Liu *et al* 2014, Gaubert *et al* 2019). Monthly time series for trend detection were selected to represent seasonal flux variabilities. The time series of the global $FFCO_2$ and NBE are shown in figure 1(b). $FFCO_2$ and NBE for the grid cell containing Beijing are shown in figure 1(c) as an example. The variation coefficient (vc, defined as the ratio of the standard deviation to the mean) for the global $FFCO_2$ is 0.3, while −6.4 for the global NBE. For Beijing, the cv is 0.11 for $FFCO_2$ and −14.2 for NBE. In both cases, NBE variation dominates the variability from $FFCO_2$.

2.2. Trend detection method

For simplicity, we define a linear trend to estimate the first-order change in the time series, as changes in $FFCO_2$ are expected to be gradual in the near future; this approach also allows for a simple comparison across different regions. The time series of observed fluxes can be defined by a simple additive noise model:

$$y(t) = F(t) + \epsilon, \quad (1)$$

where $y(t)$ are the derived fluxes at a gridded location, $F(t)$ is a function to describe how fluxes change in time, and ϵ represents the 'unexplained variability' in the system. We represent the times series as a simple model that includes a linear trend and seasonal cycle:

$$F_{SC}(t; a_0, a_1, C, D) = a_0 + a_1 t + \sum_{n=1}^{4}[C_n \sin(2n\pi t) + D_n \cos(2n\pi t)], \quad (2)$$

where t is the decimal year, a_0 and a_1 are offset and slope, C_n and D_n are coefficients for the amplitude of seasonal variations, and n represents the normalized frequency index of the harmonics-4 are chosen here. IAVs not captured by the harmonics is attributed to the unexplained variability term (ϵ). The least square method of the optimization function in the Python package scipy is used.

We use a search method that starts with a 3 year temporal window and extends 1 more year at each iteration until a significant trend emerges (defined by the p-value of a_1 being less than 0.05 for two consecutive end years). The length of this temporal window thus represents the trend detection time. We first estimate the detection time and associated trend (a_1) of the total CO_2 fluxes at each model grid cell from 2015 onward, and then, we compare the estimated total CO_2 trends with corresponding trends imbedded in $FFCO_2$ emissions to evaluate whether trends in the total fluxes are directly relevant for $FFCO_2$ in different places across the world.

3. Results

3.1. Spatial distribution of the detection time and corresponding trend

The detection time has a global median of 10 years, which means that a significant trend in the total CO_2 fluxes could be identified within a decade for over a half of the land grids (figure 2). In 4% of the grids, no significant trend emerges over the 85 simulation years. The median of detected trends in the total CO_2 fluxes are 0.9 gC m^{-2} yr^{-2}, but the spatial variations are very large (the 10th and 90th percentiles being −87.5 and 78.5 gC m^{-2} yr^{-2}). To relate these changes to anthropogenic emission variability, we also compute FFCO2 trends in the absence of the biosphere. Trends in the $FFCO_2$ component have a median of 0.4 gC m^{-2} yr^{-2}, with their 10th and 90th percentiles being 0.01 and 4.3 gC m^{-2} yr^{-2} at corresponding detection time of the total CO_2 fluxes. The magnitude of trends in the $FFCO_2$ are over a factor of 2 smaller than trends in the total CO_2 fluxes and an order of magnitude less variable. This difference is driven primarily by the IAV in NBE, in particular extreme events in the natural carbon cycle. For example, a period of successive droughts can impose a large sub-decadal trend in the total CO_2 flux that is not representative of longer-term biospheric or $FFCO_2$ fluxes. Consequently, caution must be exercised in the interpretation of short-term total CO_2 trends in regions with an active biosphere.

A regional summary of the detection time and corresponding trend is shown in figure 3. The Middle East has the shortest detection time across the globe—5 years, with the least divergence between the $FFCO_2$ ($2.5^{6.0}_{0.5}$ gC m^{-2} yr^{-2}) and the total CO_2 $4.2^{18.2}_{-2.9}$ gC m^{-2} yr^{-2}) trends (the median is reported here, with the subscript and superscript showing the 10th and 90th percentiles, respectively, hereafter). In contrast, Canada has the longest detection time (29^{85}_{5} years), followed by Russia (23^{65}_{5} years). Detection time in the tropics is not particularly long, but large divergences between the total CO_2 and $FFCO_2$ trends are found indicating that trends in the total CO_2 fluxes are induced by NBE instead of $FFCO_2$. Although the median of the total CO_2 trends in the Central and South America agree roughly with the $FFCO_2$ trends, their variability are larger by more than an order of magnitude than $FFCO_2$ ($2.4^{47.4}_{-70.4}$ and $-1.1^{59.3}_{-76.1}$ gC m^{-2} yr^{-2} for the total CO_2, whereas $0.6^{1.5}_{0.1}$ and $0.2^{0.7}_{0.02}$ gC m^{-2} yr^{-2} for the $FFCO_2$, respectively). Also, NBE from deforestation and land use changes are also important anthropogenic signals in those regions, but not addressed here. As for Southeast Asia and Oceania, the median of the total CO_2 trends also differ significantly from the $FFCO_2$ trends, as the model ensemble mean suggest enhanced land carbon sink over the corresponding total CO_2 trend detection time ($-28.7^{67.2}_{-119.8}$ and $-19.1^{17.3}_{-77.7}$ gC m^{-2} yr^{-2} for the total CO_2, whereas $1.1^{3.3}_{0.04}$ and $0.03^{0.4}_{0.01}$ gC m^{-2} yr^{-2} for the $FFCO_2$).

Each region, however, is a combination of grids with strong and weak $FFCO_2$ trends. Focusing on grids where $FFCO_2$ trends are greater than 5 gC m^{-2} yr^{-2} (~300 locations globally), approximately a third of grids show total CO_2 trends within 25% of concomitant FFCO2 trends. These trends are primarily in Eastern China, Europe, Middle East, and North America. For example, China contributes to ~25% of these large $FFCO_2$ trends. Of those, about 20% show total CO_2 trends within 25% of the $FFCO_2$ trends, while ~40% differ by more than 100%. The differences are less pronounced in the Middle East, where over 70% of total CO2 trends is within 25%. It is in this region where top-down systems may be the most effective in the near-term at a sub-decadal scale, even at a coarse resolution. We note that although the specific numbers are dependent on the current model simulations and the starting year, the spatial distribution of the relative contribution of biosphere to the detection of $FFCO_2$ trends should be robust given our current understanding of the natural carbon cycle.

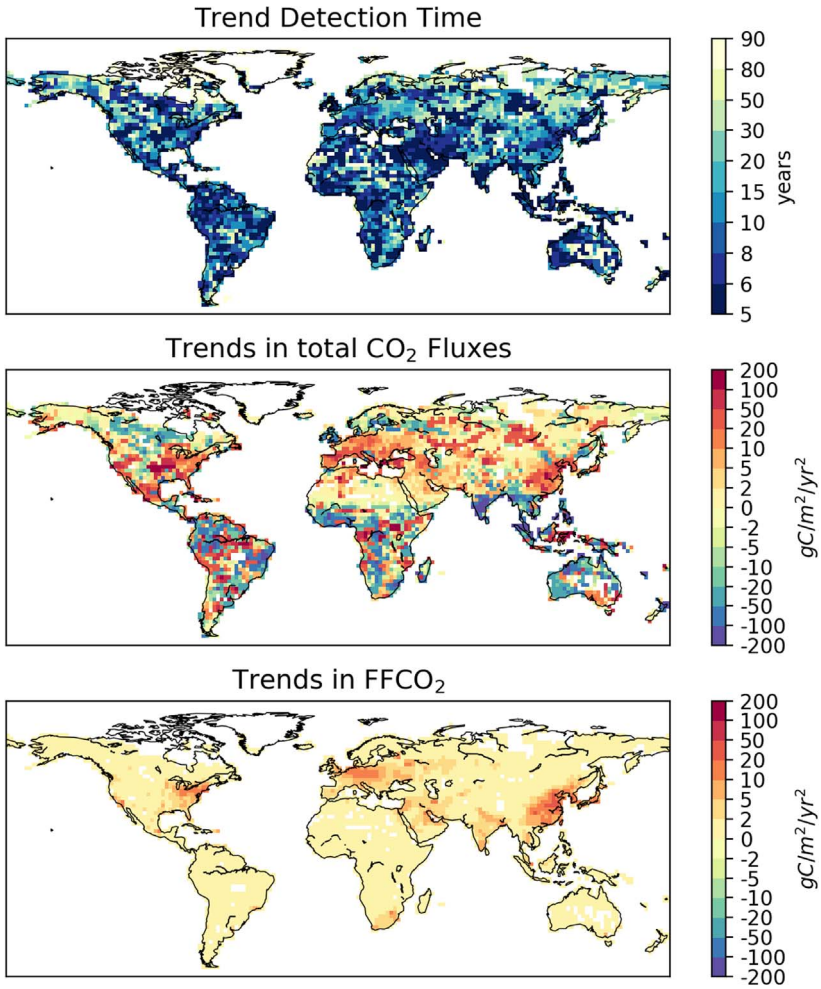

Figure 2. Spatial distribution of the trend detection time of the total CO_2 fluxes and corresponding trends in the total CO_2 fluxes and in the $FFCO_2$ component. The results are based on the modeled NBE ensemble mean.

However, we also expect that as more extensive regional monitoring networks become available, the relative weight of $FFCO_2$ and natural carbon fluxes will change when moving towards a higher spatiotemporal resolution, and hence, the signal-detection may improve upon the baselines we documented here.

3.2. Tradeoff between the detection time and the representativeness of estimated trend

The magnitude of estimated trends decreases exponentially with the increase of detection time because the trend in NBP is closer to neutral over longer time scales (figure S3). This is not surprising as short-term variations that qualify as a statistically significant trend at sub-decadal scales may not be representative of the long-term change. We further test that trends obtained using longer initial window lengths for the search method are generally of smaller magnitudes than those estimated using a shorter initial window (figure S4). Using longer initial window of 5 and 10 years result in longer median detection time of 12 and 19 years with the differences between the total CO_2 and $FFCO_2$ trends reduced to $0.13^{17.9}_{-28.6}$ and $0.21^{7.8}_{-8.9}$ gC m^{-2} yr^{-2} using 5 and 10 year windows, respectively, with 43% and 79% reductions in the 10th and 90th quantile range compared to the results using 3 year initial window ($0.22^{33.6}_{-47.4}$ gC m^{-2} yr^{-2}). Although it is preferable to monitor short-term variations of regional $FFCO_2$ emissions, this analysis indicates that the use of CO_2 observations to infer $FFCO_2$ flux changes at a relatively short time scale should be treated with caution as the variations in the NBE over a few years could confound the attribution of observed CO_2 trends even though those short-term NBE trends are not indicative of the long-term biosphere trends. A higher accuracy with longer detection time only occurs where the natural biosphere is balanced over several decades; in regions where land-use change and carbon feedbacks are important, natural trends could still dominate the total CO_2 trend (figure 2).

To isolate the role of NBE variability in shaping the distribution of trend detection time, we created a test scenario $S_{FF\_Uniform}$ in which both the emission intensity and trend in the FF fluxes are uniformly distributed in space with the global total $FFCO_2$ equal to that of RCP8.5 (figure S5). The spatial variations are

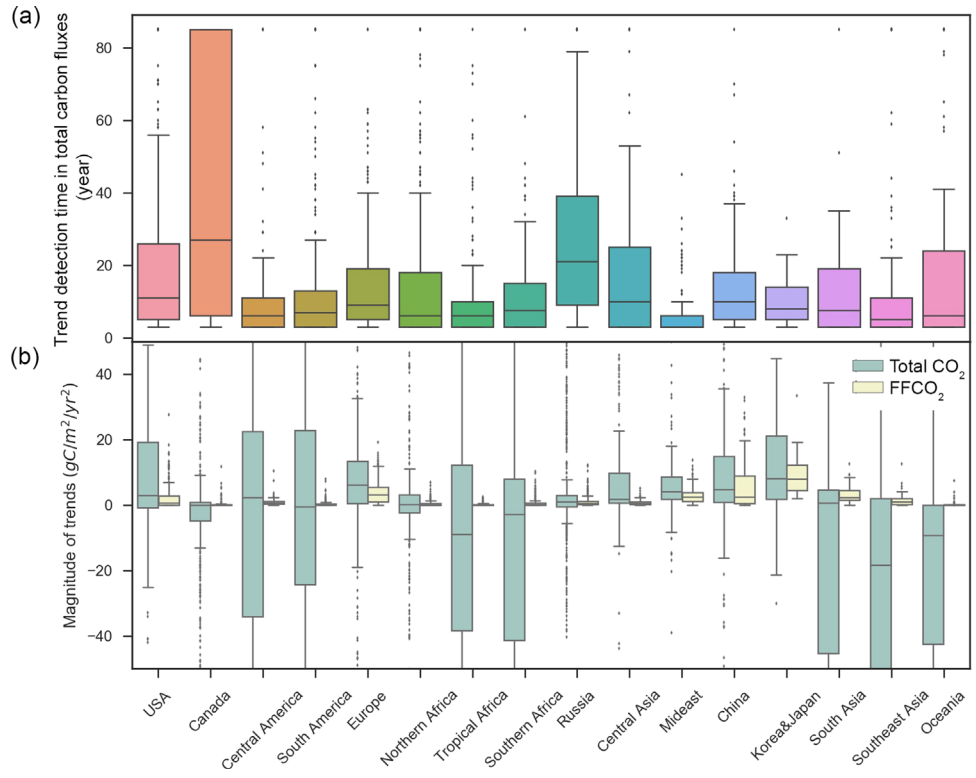

Figure 3. Regional summary of (a) trend detection time and (b) corresponding magnitude of trends in the total CO_2 fluxes and in the $FFCO_2$ component, respectively. For each region, the central rectangle spans the first quartile to the third quartile with a segment inside the rectangle showing the median; whiskers above and below the box show the minimum and maximum; outliers are noted as small dots (defined as 1.5 × interquartile range more above the third-quartile or below the first-quartile). Regional mask is shown in figure S2.

now determined by the variability and trends embedded in the NBE fluxes alone. Compared to the reference (shown in figure 2 and noted as $S_{FF\_RCP8.5}$), the detection time in $S_{FF\_Uniform}$ for trend in the total CO_2 fluxes becomes longer in regions where the original $FFCO_2$ are high, e.g. such as East Asia, India, Europe and Northeast US, while detection time shortens significantly in regions where the uniformly distributed $FFCO_2$ induce more detectable trends (figure S5). The comparison between $S_{FF\_RCP8.5}$ and $S_{FF\_Uniform}$ illuminates the interplay between FF and NBE to the detection of trends in the total CO_2 fluxes. Variability in the NBE remains to be the largest drawback of detection time. For example, the short detection time for the Middle East (less than 5 years) for both $S_{FF\_RCP8.5}$ and $S_{FF\_Uniform}$ show that low NBE in the arid regions allow FF trends to emerge more easily regardless of the choice of detection method. As for Eastern China, which has a large absolute FF emission flux in the original emission scenario, it requires a much longer detection time for the case of $S_{FF\_Uniform}$. However, future CO_2 emissions may deviate from the RCP8.5 scenario and plateau or even decrease in the future if emissions follow the Intended Nationally Determined Contributions submitted to UN Framework Convention on Climate Change. In such cases, independent constraints on the natural carbon cycle fluxes are even more critical to quantify actual changes in $FFCO_2$ fluxes.

3.3. Detection time and trends in megacities

Megacities are of particular interest because of their disproportionate impact on the anthropogenic carbon budget and we expect that future observing systems will focus on quantifying megacity emissions and trends. We use population as a criterion to focus on the grids where the top 25 mega-cities are located. Significant trends can be detected in approximately one third to a half of the cities within a decade with a monthly 2° × 2° resolution (14 out of 25; figure 4). Intuitively, cities with a relatively short detection time are associated with either a relatively large trend in FF flux (>10 gC m^{-2} yr^{-2}) or a significant trend in NBE over the detection window. For the former, trends in the total CO_2 fluxes are in good agreement with trends in the $FFCO_2$ fluxes (e.g. New York, Seoul, Los Angeles, Tokyo); whereas for the latter case, the divergences between the total CO_2 and $FFCO_2$ trends are large, in some cases differ in an order of magnitude (e.g. London, Dhaka, Sydney). There is also a large uncertainty range in the trends of the total CO_2 flux using individual ESMs, due to differences in trends embedded in each NBE simulations and in the detection time.

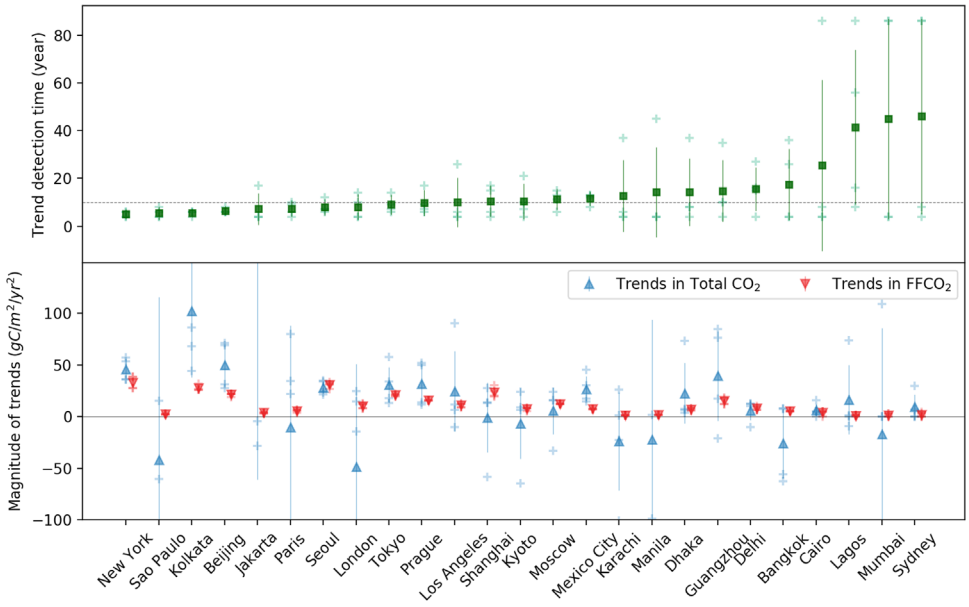

Figure 4. Results of the top 25 megacities (a) the trend detection time and (b) trends in the total CO_2 fluxes versus trends imbedded in the $FFCO_2$ at the trend detection time of the total CO_2 fluxes. Individual scatter shown in small crosses represent results using NBE simulated by different ESMs, the solid markers represent the ensemble mean and the error bars along the *y*-axis indicate standard deviations using different NEB simulations.

Overall, there are eight cities whose total CO_2 trends matches trends in the $FFCO_2$ to within 25%. Based upon these results and the detection time for both methods, we would expect that only in arid regions like Middle East, it would be possible to observe $FFCO_2$ change effectively in the near term with a CO_2—only monitoring system. Tropical regions remain a significant challenge. At $2^\circ \times 2^\circ$ degree resolution the detection time for Sao Paulo, Bangkok, and Lagos are close to a decade, the weak FF trend is masked by strong NBE trends leading to total CO_2 trends of −13, −9, and 25 gC m^{-2} yr^{-2}, respectively (comparing to $FFCO_2$ trend of 2.6, 3.5, and 1 gC m^{-2} yr^{-2}).

4. Uncertainty and perspectives

In this study, we show the spatial distribution of trend detection time of total CO_2 fluxes and how these derived total CO_2 trends are representative of the $FFCO_2$ trends at a $2^\circ \times 2^\circ$ degree with monthly data. This analysis provides us helpful information at a global scale regarding how feasible it is at a certain location to define an 'urban dome', where the background air that has a small influence from natural carbon fluxes and their associated IAVs. We note that the analysis is performed at a relatively coarse spatial resolution, which is limited by current available global NBE simulations and at the same time equivalent to global atmospheric inversions that ingest the currently available global observations. Higher resolution in both space and time would likely be achieved for city scale $FFCO_2$ studies where local CO_2 gradient between the urban center and the rural area would be the key information to quantify $FFCO_2$. Nevertheless, our analysis is relevant as urban landscapes often exhibit considerable heterogeneity in the land cover and land use, thus the mixed contribution from anthropogenic and biospheric sources will not be automatically solved with increasing spatial and temporal resolution alone. At a higher resolution, the relative contribution of $FFCO_2$ and NBE would change, e.g. it will become easier to detect $FFCO_2$ signal from the total CO_2 fluxes if the magnitude of $FFCO_2$ fluxes outweigh the NBE over the estimated domain, as we illustrate here using different $FFCO_2$ scenarios. Still, for cases where a clear 'urban dome' could be identified, inter-annual variations in the NBE of the background region could be aliased into the $FFCO_2$ trend estimates if they are not adequately considered. For instance, an increase in the CO_2 enhancement over the urban dome could result from an increase in the city $FFCO_2$ or an increase in the net carbon uptake by the suburban vegetation.

As we expect to monitor progressive changes in $FFCO_2$, trend detection is an efficient way to define the relative change and whether a certain region is on track of the promised emission reduction trajectory. However, a linear trend determined with a statistical model has limited skill in representing non-monotonic or nonlinear changes and is sensitive to the starting and ending points. In addition, a regular seasonal cycle we considered here may not model well ecosystems without regular seasonality (e.g. ecosystem with larger variations in the onset of dry and wet seasons). Nevertheless, our simple approach derives a global reference for regionally specific studies prior to the establishment of global, but fine-scale detailed observations. Our sensitively test starting from

random years instead of 2015 to test the sensitivity of the starting point suggest the resultant global pattern being quite robust. Our test using different length of the initial searching window also confirm this point.

This analysis highlighted, on the one hand, a few regions that are feasible for using top-down $FFCO_2$ constraints, and on the other hand, the difficulty of disentangling $FFCO_2$ changes from the natural carbon cycle with CO_2 observations alone. Therefore, multiple pieces of information will be needed to observe regional $FFCO_2$ trend accurately. For instance, periodic ^{14}C measurements (Basu *et al* 2016, Wang *et al* 2017) and the combination of other fossil fuel tracers (e.g. NO_2, CO) could bring in additional information even though there are complications due to the variation and uncertainty in their emission factor ratio to CO_2 and by atmospheric chemistry (Gamnitzer *et al* 2006, Rayner *et al* 2014). In addition, proxies to constrain the terrestrial ecosystem production (e.g. solar induced fluorescence and carbonyl sulfide, OCS) could also contribute essential information by adding more constraints to different components of the carbon cycle to estimate the progress of climate mitigation (Schimel *et al* 2015, Bloom *et al* 2016, Bowman *et al* 2017, Liu *et al* 2017, Sellers *et al* 2018). Also, many countries also invoke land use management for their National Determined Contributions (Grassi *et al* 2017), thus monitoring corresponding biospheric fluxes remains highly relevant. Furthermore, from the inventory viewpoint, indicators to track emission activity and technology development are also important (Peters *et al* 2017a). With increasing spatial-temporal resolution and coverage of the above-mentioned features (Broquet *et al* 2018), a data assimilation scheme that includes consideration for both $FFCO_2$ and NBE uncertainties and integrates multiple observational streams will help to account for variations in these two fluxes consistently.

5. Conclusion

Our results provide an initial assessment of the trend detection time and associated trends in the gridded total CO_2 fluxes over the globe with synthetic fluxes from CMIP5 under the assumption of an idealized CO_2 observing and attribution system that can derive such fluxes. The trend detection time for gridded total CO_2 has a median of 10 years at a resolution of $2^\circ \times 2^\circ$ degree using monthly flux data, with large spreads depending on fossil fuel emission magnitude versus NBE variability. The differences between trends in the total CO_2 fluxes and in the underlying $FFCO_2$ component highlight the role of natural carbon cycle variability in modulating regional detection of $FFCO_2$ emission trends using CO_2 observations alone, particularly in the tropics and subtropics where mega-cities with large populations are emerging and developing rapidly. As we have shown, using CO_2 flux estimates alone at such a resolution can only quantify fossil fuel trends in a few places—mostly limited to the arid region. Monitoring $FFCO_2$ at a city scale with a finer spatial resolution may become easier when the magnitude of $FFCO_2$ fluxes outweigh the NBE variations. However, these local estimates will still need to be integrated with regional, national, and ultimately global estimates of natural and anthropogenic carbon. Consequently, it will be important to constrain the background biosphere fluxes so that their uncertainties are not aliased into the $FFCO_2$ estimates. Therefore, the challenge of assessing international carbon mitigation progress requires an approach linking both bottom-up and top-down estimates within an assimilation and attribution system that integrates information on both natural and anthropogenic carbon fluxes.

Acknowledgments

The authors are very grateful to the CMIP5 project and ESG Federation for making ESM simulations publicly available. The research was supported by the NASA CMS-Flux project NNH16ZDA001N-CMS and a NASA Postdoctoral Program fellowship award to Y Yin. The research was carried out, in part, at the Jet Propulsion Laboratory, California Institute of Technology, under a contract with the National Aeronautics and Space Administration.

ORCID iDs

Yi Yin https://orcid.org/0000-0003-4750-4997
Kevin Bowman https://orcid.org/0000-0002-8659-1117

References

Andres R J, Boden T A and Higdon D 2014 A new evaluation of the uncertainty associated with CDIAC estimates of fossil fuel carbon dioxide emission *Tellus* B **66** 23616

Basu S, Miller J B and Lehman S 2016 Separation of biospheric and fossil fuel fluxes of CO_2 by atmospheric inversion of CO_2 and $14CO_2$ measurements: observation system simulations *Atmos. Chem. Phys.* **16** 5665–83

Battersby S 2018 News feature: the carbon detectives *Proc. Natl Acad. Sci. USA* **115** 6873–7

Bloom A A, Exbrayat J-F, van der Velde I R, Feng L and Williams M 2016 The decadal state of the terrestrial carbon cycle: global retrievals of terrestrial carbon allocation, pools, and residence times *Proc. Natl Acad. Sci. USA* **113** 1285–90

Bowman K W *et al* 2017 Global and Brazilian carbon response to El Niño Modoki 2011–2010 *Earth Space Sci.* **4** 637–60

Broquet G, Bréon F-M, Renault E, Buchwitz M, Reuter M, Bovensmann H, Chevallier F, Wu L and Ciais P 2018 The potential of satellite spectro-imagery for monitoring CO_2 emissions from large cities *Atmos. Meas. Tech.* **11** 681–708

Buchwitz M *et al* 2018 Copernicus Climate Change Service (C3S) global satellite observations of atmospheric carbon dioxide and methane *Adv. Astronaut. Sci. Technol.* **1** 57–60

Chevallier F *et al* 2010 CO_2 surface fluxes at grid point scale estimated from a global 21 year reanalysis of atmospheric measurements *J. Geophys. Res.* **115** D21307

Crisp D 2018 A constellation architecture for monitoring carbon dioxide and methane from space (http://ceos.org/document_management/Virtual_Constellations/ACC/Documents/CEOS_AC-VC_GHG_White_Paper_Version_1_20181009.pdf)
Duren R M and Miller C E 2012 Measuring the carbon emissions of megacities *Nat. Clim. Change* **2** 560–2
Francey R J *et al* 2013 Atmospheric verification of anthropogenic CO_2 emission trends *Nat. Clim. Change* **3** 520–4
Friedlingstein P, Meinshausen M, Arora V K, Jones C D, Anav A, Liddicoat S K and Knutti R 2014 Uncertainties in CMIP5 climate projections due to carbon cycle feedbacks *J. Clim.* **27** 511–26
Gamnitzer U, Karstens U, Kromer B, Neubert R E M, Meijer H A J, Schroeder H and Levin I 2006 Carbon monoxide: a quantitative tracer for fossil fuel CO_2? *J. Geophys. Res.* **111** D22302
Gaubert B *et al* 2019 Global atmospheric CO_2 inverse models converging on neutral tropical land exchange but diverging on fossil fuel and atmospheric growth rate *Biogeosci.* **16** 117–34
Grassi G, House J, Dentener F, Federici S, den Elzen M and Penman J 2017 The key role of forests in meeting climate targets requires science for credible mitigation *Nat. Clim. Change* **7** 220–6
Gurney K R *et al* 2002 Towards robust regional estimates of CO_2 sources and sinks using atmospheric transport models *Nature* **415** 626–30
Hoffman F M *et al* 2014 Causes and implications of persistent atmospheric carbon dioxide biases in Earth System Models *J. Geophys. Res. Biogeosci.* **119** 141–62
Hutyra L R, Duren R, Gurney K R, Grimm N, Kort E A, Larson E and Shrestha G 2014 Urbanization and the carbon cycle: current capabilities and research outlook from the natural sciences perspective *Earth's Future* **2** 473–95
IPCC 2013 *Climate Change 2013. The Physical Science Basis. Working Group I Contribution to the Fifth Assessment Report of the Intergovernmental Panel on Climate Change* (Cambridge: Cambridge University Press)
Kort E A, Frankenberg C, Miller C E and Oda T 2012 Space-based observations of megacity carbon dioxide *Geophys. Res. Lett.* **39** L17806
Lauvaux T *et al* 2016 High-resolution atmospheric inversion of urban CO_2 emissions during the dormant season of the indianapolis flux experiment (INFLUX) *J. Geophys. Res. Atmos.* **121** 5213–36
Le Quéré C *et al* 2016 Global carbon budget 2016 *Earth Syst. Sci. Data* **8** 605–49
Le Quéré C *et al* 2018 Global carbon budget 2017 *Earth Syst. Sci. Data* **10** 405–48
Liu J *et al* 2014 Carbon monitoring system flux estimation and attribution: impact of ACOS-GOSAT X CO_2 sampling on the inference of terrestrial biospheric sources and sinks *Tellus* B **66** 22486
Liu J *et al* 2017 Contrasting carbon cycle responses of the tropical continents to the 2015-2016 El Niño *Science* **358** eaam5690
McKain K, Wofsy S C, Nehrkorn T, Eluszkiewicz J, Ehleringer J R and Stephens B B 2012 Assessment of ground-based atmospheric observations for verification of greenhouse gas emissions from an urban region *Proc. Natl Acad. Sci. USA* **109** 8423–8
Mitchell L E *et al* 2018 Long-term urban carbon dioxide observations reveal spatial and temporal dynamics related to urban characteristics and growth *Proc. Natl Acad. Sci. USA* **115** 2912–7
Nassar R, Hill T G, McLinden C A, Wunch D, Jones D B A and Crisp D 2017 Quantifying CO_2 emissions from individual power plants from space *Geophys. Res. Lett.* **44** 10045–53
National Research Council 2010 *Verifying Greenhouse Gas Emissions: Methods to Support International Climate Agreements* (Washington, DC: National Academies Press) (https://doi.org/10.17226/12883)
O'Brien D M, Polonsky I N, Utembe S R and Rayner P J 2016 Potential of a geostationary geoCARB mission to estimate surface emissions of CO_2, CH_4, and CO in a polluted urban environment: case study Shanghai *Atmos. Meas. Tech.* **9** 4633–54
Peters G P *et al* 2017b Towards real-time verification of CO_2 emissions *Nat. Clim. Change* **7** 848–50
Peters G P, Andrew R M, Canadell J G, Fuss S, Jackson R B, Korsbakken J I, Le Quéré C and Nakicenovic N 2017a Key indicators to track current progress and future ambition of the Paris agreement *Nat. Clim. Change* **7** 118–22
Peters W *et al* 2007 An atmospheric perspective on North American carbon dioxide exchange: carbon tracker *Proc. Natl Acad. Sci.* **104** 18925–30
Peylin P *et al* 2013 Global atmospheric carbon budget: results from an ensemble of atmospheric CO_2 inversions *Biogeosciences* **10** 6699–720
Pillai D, Buchwitz M, Gerbig C, Koch T, Reuter M, Bovensmann H, Marshall J and Burrows J P 2016 Tracking city CO_2 emissions from space using a high-resolution inverse modelling approach: a case study for Berlin, Germany *Atmos. Chem. Phys.* **16** 9591–610
Polonsky I N, O'Brien D M, Kumer J B and O'Dell C W 2014 Performance of a geostationary mission, geoCARB, to measure CO_2, CH_4 and CO column-averaged concentrations *Atmos. Meas. Tech.* **7** 959–81
Rayner P J, Utembe S R and Crowell S 2014 Constraining regional greenhouse gas emissions using geostationary concentration measurements: a theoretical study *Atmos. Meas. Tech.* **7** 3285–93
Rödenbeck C, Houweling S, Gloor M and Heimann M 2003 CO_2 flux history 1982–2001 inferred from atmospheric data using a global inversion of atmospheric transport *Atmos. Chem. Phys.* **3** 1919–64
Schimel D, Pavlick R, Fisher J B, Asner G P, Saatchi S, Townsend P, Miller C, Frankenberg C, Hibbard K and Cox P 2015 Observing terrestrial ecosystems and the carbon cycle from space *Glob. Change Biol.* **21** 1762–76
Schwandner F M *et al* 2017 Spaceborne detection of localized carbon dioxide sources *Science* **358** eaam5782
Sellers P J, Schimel D S, Moore B, Liu J and Eldering A 2018 Observing carbon cycle-climate feedbacks from space *Proc. Natl Acad. Sci. USA* **115** 7860–8
Shiga Y P, Michalak A M, Gourdji S M, Mueller K L and Yadav V 2014 Detecting fossil fuel emissions patterns from subcontinental regions using North American *in situ* CO_2 measurements *Geophys. Res. Lett.* **41** 4381–8
Staufer J *et al* 2016 The first 1 year long estimate of the Paris region fossil fuel CO_2 emissions based on atmospheric inversion *Atmos. Chem. Phys.* **16** 14703–26
Taylor K E, Stouffer R J and Meehl G A 2012 An overview of CMIP5 and the experiment design *Bull. Am. Meteorol. Soc.* **93** 485–98
Turner A J, Shusterman A A, McDonald B C, Teige V, Harley R A and Cohen R C 2016 Network design for quantifying urban CO_2 emissions: assessing trade-offs between precision and network density *Atmos. Chem. Phys.* **16** 13465–75
Verhulst K R *et al* 2017 Carbon dioxide and methane measurements from the Los Angeles megacity carbon project: I. Calibration, urban enhancements, and uncertainty estimates *Atmos. Chem. Phys.* **17** 8313–41
Wang Y, Broquet G, Ciais P, Chevallier F, Vogel F, Kadygrov N, Wu L, Yin Y, Wang R and Tao S 2017 Estimation of observation errors for large-scale atmospheric inversion of CO_2 emissions from fossil fuel combustion *Tellus* B **69** 1325723
Wu K, Lauvaux T, Davis K J, Deng A, Lopez Coto I, Gurney K R and Patarasuk R 2018 Joint inverse estimation of fossil fuel and biogenic CO_2 fluxes in an urban environment: an observing system simulation experiment to assess the impact of multiple uncertainties *Elem. Sci. Anth.* **6** 17
Wu L, Broquet G, Ciais P, Bellassen V, Vogel F, Chevallier F, Xueref-Remy I and Wang Y 2016 What would dense atmospheric observation networks bring to the quantification of city CO_2 emissions? *Atmos. Chem. Phys.* **16** 7743–71